



HAL
open science

Enhancement of multifiber beam elements in the case of reinforced concrete structures for taking into account the lateral confinement of concrete due to stirrup

N Khoder, S. Grange, Y. Sieffert

► To cite this version:

N Khoder, S. Grange, Y. Sieffert. Enhancement of multifiber beam elements in the case of reinforced concrete structures for taking into account the lateral confinement of concrete due to stirrup. EURO-C 2018, Feb 2018, Bad Hofgastein, Austria. hal-02004330

HAL Id: hal-02004330

<https://hal.science/hal-02004330>

Submitted on 1 Feb 2019

HAL is a multi-disciplinary open access archive for the deposit and dissemination of scientific research documents, whether they are published or not. The documents may come from teaching and research institutions in France or abroad, or from public or private research centers.

L'archive ouverte pluridisciplinaire **HAL**, est destinée au dépôt et à la diffusion de documents scientifiques de niveau recherche, publiés ou non, émanant des établissements d'enseignement et de recherche français ou étrangers, des laboratoires publics ou privés.

Enhancement of multifiber beam elements in the case of reinforced concrete structures for taking into account the lateral confinement of concrete due to stirrup

N. Khoder

Univ. Grenoble Alpes, CNRS, Grenoble INP, 3SR, 38000 Grenoble, France

S. Grange

Univ Lyon, INSA-LYON, GEOMAS, F-69621, Villeurbanne, France

Y. Sieffert

Univ. Grenoble Alpes, CNRS, Grenoble INP, 3SR, 38000 Grenoble, France

ABSTRACT: Many researches have been conducted in the structural engineering field in order to develop efficient numerical tools able to reproduce the complex nonlinear behavior of reinforced concrete structures. In the case of slender elements, enhanced beam models have been developed to try to introduce shear effects, but in these models, the transverse steel is sometimes taken into consideration with approximated manner or often not at all. However, as shown by some experimental tests, the amount of transverse reinforcement triggers significantly the behavior of beam elements, especially under cyclic loading. The present study addresses this problem by investigating solutions for an enhanced multifiber beam element, accounting for vertical stretching of the cross-section occurring due to the presence of stirrups. A timoshenko beam element with internal degrees of freedom and higher order interpolation functions is selected. Full 3D stresses and strains are obtained and the construction of the element and sectional stiffness matrices is detailed. The element presented hereafter is suitable for an arbitrary shape cross-section made of heterogeneous materials. Numerical applications on a plain concrete cantilever beam subjected to tension and bending tests respectively are presented. Moreover, as a first application, a dilation effect is added to the concrete fibers in order to highlight the role of transversal rebars. All the numerical results are confronted to the outcomes of standard 3D finite element computations.

1 INTRODUCTION

To study the seismic vulnerability of existing reinforced concrete structures, numerical computations at the structural scale able to account for material nonlinearities are needed. 2D and 3D finite element formulations are too costly, whereas multifiber beam elements combine the advantages of high computational speed with an increased accuracy for nonlinear materials. The principle of multifiber modelling consists on adding a two dimensional section at the Gauss point of the element. Each section is afterwards discretized into several elements presenting Gauss points where stresses and strains are computed. To this end, generalized strains are obtained at the beam Gauss points from the node displacements. Then, based upon Euler-Bernoulli or Timoshenko's theory, they are used to calculate the total strains, and with an adequate constitutive law, stresses are deduced at the

Gauss points of the section. The generalized forces are finally derived after an integration made over the cross-section (Guedes et al. 1994).

A variety of approaches have been developed to try to introduce shear effects, such as those proposed by (Le Corvec 2012), but whose model can't be applied to reinforced concrete elements, and the numerical formulation of (Mohr et al. 2010) which is adapted to reinforced concrete applications but works only in 2D. More recently, (Capdevielle et al. 2016) developed a nonlinear multifiber beam model which provides robust results by the introduction of torsional warping in the case of reinforced concrete beams subjected to shear dominating loads.

In the above mentioned works, the transverse steel is sometimes taken into consideration with approximated manner or often not at all. However, as shown by some experimental tests conducted by Cusson & Paultre (1995), the amount of transverse reinforce-

ment triggers significantly the behavior of beam elements, especially under cyclic loading.

Hereafter, a 3D enhanced multifiber beam model able to account for the distortion of the section is presented. It's a displacement-based formulation and higher order interpolation functions are involved in order to avoid shear locking problems. Moreover, longitudinal and transversal rebars are introduced in the numerical model and their implementation is validated by comparisons performed with results of 3D finite element calculations in the linear elastic framework.

2 PROPOSED MODEL

2.1 Section Kinematics

A 3D multifiber Timoshenko beam, displacement-based, element has been developed. The main assumption considered herein is that the full displacement of any fiber at the cross-section level is defined by the superposition of the traditional rigid body displacements of the plane section (\mathbf{u}^P) obtained with Timoshenko's theory, plus an additional displacement field (\mathbf{u}^w). The latter one has two transversal components, u_y^w and u_z^w , which stand for the distortion of the section in y and z directions respectively. The total displacement (\mathbf{u}) of any fiber is given by the following equation:

$$\mathbf{u} = \underbrace{\begin{bmatrix} U_x(x) - y\theta_z(x) + z\theta_y(x) \\ U_y(x) - z\theta_x(x) \\ U_z(x) + y\theta_x(x) \end{bmatrix}}_{\mathbf{u}^P} + \underbrace{\begin{bmatrix} 0 \\ u_y^w(x, y, z) \\ u_z^w(x, y, z) \end{bmatrix}}_{\mathbf{u}^w} \quad (1)$$

U_x , U_y and U_z being the translations in x, y and z directions respectively. As for θ_x , θ_y and θ_z , they denote the three rotations about x, y and z axes respectively, for a standard 3D beam element.

Under the assumption of small displacements, the total strain at any point will be formed by the sum of the plane strain field (ϵ^P) and the distortional strain (ϵ^w) as follows:

$$\epsilon = \frac{1}{2} (\text{grad}(\mathbf{u}) + \text{grad}(\mathbf{u}))^T = \epsilon^P(\mathbf{u}^P) + \epsilon^w(\mathbf{u}^w) \quad (2)$$

Therefore, the 6 components of the total strain field are defined as:

$$\begin{cases} \epsilon_{xx} = \frac{dU_x}{dx} - y \frac{d\theta_z}{dx} + z \frac{d\theta_y}{dx} \\ \epsilon_{yy} = \frac{\partial u_y^w}{\partial y} \\ \epsilon_{zz} = \frac{\partial u_z^w}{\partial z} \\ \gamma_{xy} = -\theta_z + \frac{dU_y}{dx} - z \frac{d\theta_x}{dx} + \frac{\partial u_y^w}{\partial x} \\ \gamma_{xz} = \theta_y + \frac{dU_z}{dx} + y \frac{d\theta_x}{dx} + \frac{\partial u_z^w}{\partial x} \\ \gamma_{yz} = \frac{\partial u_y^w}{\partial z} + \frac{\partial u_z^w}{\partial y} \end{cases} \quad (3)$$

With equation (3), the plane strain field can be expressed in function of the generalized deformation vector e_s , and a compatibility matrix $\mathbf{a}_s(y, z)$ so that ϵ^P takes the following form:

$$\epsilon^P = \underbrace{\begin{bmatrix} 1 & 0 & 0 & 0 & +z & -y \\ 0 & 0 & 0 & 0 & 0 & 0 \\ 0 & 0 & 0 & 0 & 0 & 0 \\ 0 & 1 & 0 & -z & 0 & 0 \\ 0 & 0 & 1 & y & 0 & 0 \\ 0 & 0 & 0 & 0 & 0 & 0 \end{bmatrix}}_{\mathbf{a}_s(y, z)} \underbrace{\begin{bmatrix} \frac{dU_x}{dx} \\ \frac{dU_y}{dx} - \theta_z \\ \frac{dU_z}{dx} + \theta_y \\ \frac{d\theta_x}{dx} \\ \frac{d\theta_y}{dx} \\ \frac{d\theta_z}{dx} \end{bmatrix}}_{e_s} \quad (4)$$

Also, as can be seen from equation (3), the distortional displacement (\mathbf{u}^w) contributes to the lateral deformation components (ϵ_{yy}) and (ϵ_{zz}). Therefore, transverse strains are not null, and the additional strains (ϵ^w) play an important role in the description of the vertical stretching of the section. As a consequence, the effect of transversal reinforcement described by lateral expansion and contraction, can be taken into account. Hence, the behavior of confined reinforced concrete elements can be studied.

2.2 Caillerie's Timoshenko beam element with internal degrees of freedom

In order to avoid shear locking problems (Stolarski and Belytschko 1982, Ibrahimbergović and Frey 1993) coming from the use of linear interpolation functions, several authors have developed numerical models based on higher order interpolation functions or functions depending on material properties. However, the latter ones present the disadvantage of not being updated after damage. Recently, a new multifiber beam element has been developed by Caillerie et al. (2015) and has been chosen to be introduced in our model. It is presented by Figure 1.

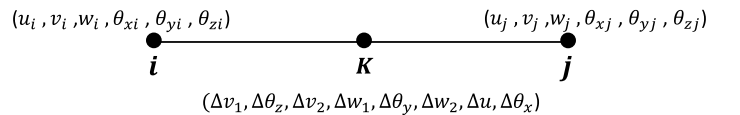


Figure 1: Definition of the degrees of freedom in the 3D version of Caillerie's beam element

Each of the two nodes (i and j) has 6 degrees of freedom: 3 translations (u, v, w) and 3 rotations ($\theta_x, \theta_y, \theta_z$) about x, y and z axes respectively. The proposed element was developed by Caillerie et al. (2015) for 2D applications and was extended in our model to a 3D formulation. Therefore, it presents an internal node K, with 8 internal degrees of freedom ($\Delta v_1, \Delta v_2, \Delta w_1, \Delta w_2, \Delta \theta_x, \Delta \theta_y, \Delta \theta_z$ and Δu).

The generalized displacement field can be therefore written as:

$$\begin{cases} U_x = N_1 u_i + N_2 \Delta u + N_3 u_j \\ U_y = H_R^1 v_i + L_R^1 \Delta v_1 + L_R^2 \Delta v_2 + H_R^2 v_j \\ U_z = H_R^1 w_i + L_R^1 \Delta w_1 + L_R^2 \Delta w_2 + H_R^2 w_j \\ \theta_x = N_1 \theta_{xi} + N_2 \Delta \theta_x + N_3 \theta_{xj} \\ \theta_y = L_R^1 \theta_{yi} + M_R^3 \Delta \theta_y + L_R^2 \theta_{yj} \\ \theta_z = L_R^1 \theta_{zi} + M_R^3 \Delta \theta_z + L_R^2 \theta_{zj} \end{cases}$$

(N_1, N_2, N_3) and (L_R^1, L_R^2, M_R^3) are defined as quadratic interpolation functions, whereas cubic shape functions $(H_R^1, H_R^2, L_R^1, L_R^2)$ are used for transverse displacements. It's worth mentioning that these higher order interpolation functions are independent of material properties. They are calculated at the beam Gauss points and take the following form:

$$\begin{aligned} N_1 &= \frac{1}{2}\xi(\xi - 1) & L_R^1 &= \frac{(\xi-1)^2(\xi+1)}{4} \\ N_2 &= 1 - \xi^2 & L_R^2 &= \frac{(\xi-1)(\xi+1)^2}{4} \\ N_3 &= \frac{1}{2}\xi(\xi + 1) & L_R^1 &= \frac{(\xi-1)(3\xi+1)}{4} \\ H_R^1 &= \frac{(\xi-1)^2(\xi+2)}{4} & L_R^2 &= \frac{(\xi+1)(3\xi-1)}{4} \\ H_R^2 &= -\frac{(\xi-2)(\xi+1)^2}{4} & M_R^3 &= 1 - \xi^2 \end{aligned} \quad (5)$$

All degrees of freedom are collected in a column vector \mathbf{U}^e structured as follows:

$$\mathbf{U}^e = [\mathbf{U}_i^{eT} \quad \Delta \mathbf{U}^{eT} \quad \mathbf{U}_j^{eT}]^T \quad (6)$$

such as:

$$\begin{aligned} \mathbf{U}_i^e &= [u_i, v_i, w_i, \theta_{xi}, \theta_{yi}, \theta_{zi}]^T \\ \Delta \mathbf{U}^e &= [\Delta v_1, \Delta \theta_z, \Delta v_2, \Delta w_1, \Delta \theta_y, \Delta w_2, \Delta u, \Delta \theta_x]^T \\ \mathbf{U}_j^e &= [u_j, v_j, w_j, \theta_{xj}, \theta_{yj}, \theta_{zj}]^T \end{aligned} \quad (7)$$

As a consequence, the generalized strain field \mathbf{e}_s can be written in function of a matrix \mathbf{B}_p which gathers the derivatives of the above mentioned interpolation functions related to longitudinal spatial discretization. Then, the new expression of the plane strain field ϵ^P becomes:

$$\epsilon^P = \mathbf{a}_s(y, z) \mathbf{B}_p \mathbf{U}^e \quad (8)$$

2.3 Distortional displacement field interpolation

It is assumed that the distortional displacement (\mathbf{u}^w) has two non-zero components in y and z directions

accounting for the vertical stretching of the cross-section. It is defined as:

$$\mathbf{u}^w(x, y, z) = [0 \quad u_y^w(x, y, z) \quad u_z^w(x, y, z)] \quad (9)$$

Where:

$$\begin{cases} u_x^w(x, y, z) = 0 \\ u_y^w(x, y, z) = c_1(x) \varphi_1(y, z) \\ u_z^w(x, y, z) = c_2(x) \varphi_2(y, z) \end{cases} \quad (10)$$

The interpolation is performed independently along the beam axis with the quadratic functions $c_1(x)$ and $c_2(x)$, and on the cross-section with functions $\varphi_1(y, z)$ and $\varphi_2(y, z)$. The latter ones are the classical quadratic functions used for 6 nodes triangular elements TRI6 and they are computed at the section Gauss points.

Distortional strains components can be therefore presented as follows:

$$\begin{cases} \epsilon_{xx}^w = \frac{\partial u_x^w}{\partial x} = 0 \\ \epsilon_{yy}^w = \frac{\partial u_y^w}{\partial y} = c_1(x) \frac{\partial \varphi_1}{\partial y} \\ \epsilon_{zz}^w = \frac{\partial u_z^w}{\partial z} = c_2(x) \frac{\partial \varphi_2}{\partial z} \\ \gamma_{xy}^w = \frac{\partial u_x^w}{\partial y} + \frac{\partial u_y^w}{\partial x} = \frac{dc_1}{dx} \varphi_1 \\ \gamma_{xz}^w = \frac{\partial u_x^w}{\partial z} + \frac{\partial u_z^w}{\partial x} = \frac{dc_2}{dx} \varphi_2 \\ \gamma_{yz}^w = \frac{\partial u_y^w}{\partial z} + \frac{\partial u_z^w}{\partial y} = c_1(x) \frac{\partial \varphi_1}{\partial z} + c_2(x) \frac{\partial \varphi_2}{\partial y} \end{cases} \quad (11)$$

The enhanced strain field can be given by the following expression:

$$\epsilon^w = \mathbf{a}_w(y, z) \mathbf{e}_w = \mathbf{a}_w(y, z) \mathbf{B}_w \mathbf{W}^e \quad (12)$$

And by the use of a matrix notation, ϵ^w becomes:

$$\epsilon^w = \begin{bmatrix} \epsilon_{xx}^w \\ \epsilon_{yy}^w \\ \epsilon_{zz}^w \\ \gamma_{xy}^w \\ \gamma_{xz}^w \\ \gamma_{yz}^w \end{bmatrix} = \underbrace{\begin{bmatrix} 0 & 0 & 0 & 0 \\ 0 & 0 & \frac{\partial \varphi_1}{\partial y} & 0 \\ 0 & 0 & 0 & \frac{\partial \varphi_2}{\partial z} \\ \varphi_1 & 0 & 0 & 0 \\ 0 & \varphi_2 & 0 & 0 \\ 0 & 0 & \frac{\partial \varphi_1}{\partial z} & \frac{\partial \varphi_2}{\partial y} \end{bmatrix}}_{\mathbf{a}_w(y, z)} \underbrace{\begin{bmatrix} \frac{dc_1}{dx} \\ \frac{dc_2}{dx} \\ c_1 \\ c_2 \end{bmatrix}}_{\mathbf{e}_w} \quad (13)$$

The matrix \mathbf{B}_w collects the longitudinal interpolation functions and their derivatives. As for the vector \mathbf{W}^e , it gathers all the distortional degrees of freedom of the points located on the section i of each element. They are treated as global DOFs of the beam element as shown by Figure 2.

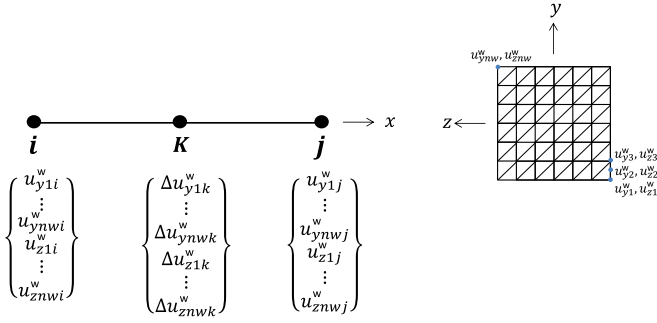


Figure 2: Distribution of the distortional degrees of freedom

Hence,

$$\mathbf{W}^e = [\mathbf{W}_{y_i}^{eT}, \mathbf{W}_{z_i}^{eT}, \Delta \mathbf{W}_y^T, \Delta \mathbf{W}_z^T, \mathbf{W}_{y_j}^{eT}, \mathbf{W}_{z_j}^{eT}]^T \quad (14)$$

With:

$$\begin{aligned} \mathbf{W}_{y(i,j)}^e &= [u_{y1(i,j)}^w \cdots u_{ymw(i,j)}^w]^T \\ \mathbf{W}_{z(i,j)}^e &= [u_{z1(i,j)}^w \cdots u_{znw(i,j)}^w]^T \\ \Delta \mathbf{W}_{(y,z)} &= [\Delta u_{(y,z)1}^w \cdots \Delta u_{(y,z)nw}^w]^T \end{aligned} \quad (15)$$

n_w being the total number of the nodes per section.

Once, the plane strain ϵ^P and the distortional strain fields ϵ^w computed at the Gauss points of the section, the stress distribution at the concrete fibers is deduced.

3 Gauss points per element are needed in order to correctly integrate the higher order polynomials, which means 3 sections per element. Thus, the calculation procedure can be illustrated by Figure 3.

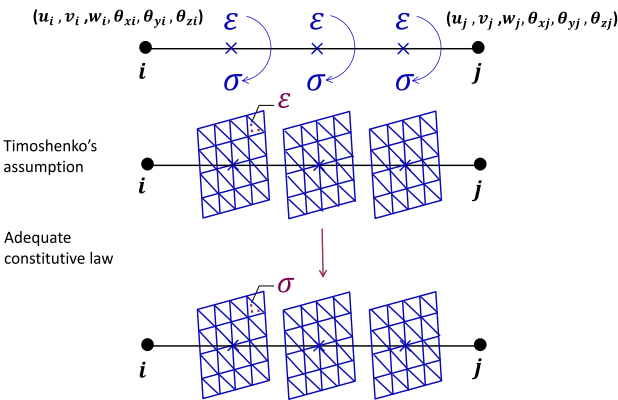


Figure 3: Calculation Procedure

3 GOVERNING EQUATIONS

Beam equilibrium is written in its weak form by equation (16). In addition, the plane section displacement

\mathbf{u}^P and the distortion one \mathbf{u}^w assumed to be orthogonal, the projection of the weak form equilibrium on these two subspaces lead to two equilibrium equations (17). The first one representing the classical equilibrium of the beam element, and the second one being the equilibrium equation of the cross-section. \mathbf{F} denotes the external forces and \mathbf{P}^w the forces coming from constrained distortion at the beam ends.

$$\int_{\Omega} \epsilon^{*T} \sigma d\Omega = \mathbf{U}^{*T} \mathbf{F}_{ext} \quad (16)$$

$$\Leftrightarrow \begin{cases} \int_{\Omega} \delta \epsilon^{P^T} \hat{\sigma}(\epsilon^P, \epsilon^w) d\Omega = \mathbf{F} \\ \int_{\Omega} \delta \epsilon^{w^T} \hat{\sigma}(\epsilon^P, \epsilon^w) d\Omega = \mathbf{P}^w \end{cases} \quad (17)$$

At the element level, the beam is discretized into n_e Timoshenko beam elements, of length l_e , each having 3 Gauss points, i.e. 3 sections, whose contribution should be summed in order to compute the terms of the element force vector \mathbf{P}_e and the element stiffness matrix \mathbf{K}_e .

Therefore, the expression of the element stiffness matrix is given by:

$$\mathbf{K}_e = \begin{bmatrix} \mathbf{K}_{pp} & \mathbf{K}_{pw} \\ \mathbf{K}_{wp} & \mathbf{K}_{ww} \end{bmatrix} \quad (18)$$

Where:

$$\begin{aligned} \mathbf{K}_{pp} &= \int_{l_e} \mathbf{B}_p^T \mathbf{a}_s^T \mathbf{K}_m \mathbf{a}_s \mathbf{B}_p dx \\ \mathbf{K}_{pw} &= \int_{l_e} \mathbf{B}_p^T \mathbf{a}_s^T \mathbf{K}_m \mathbf{a}_w \mathbf{B}_w dx \\ \mathbf{K}_{wp} &= \int_{l_e} \mathbf{B}_w^T \mathbf{a}_w^T \mathbf{K}_m \mathbf{a}_s \mathbf{B}_p dx \\ \mathbf{K}_{ww} &= \int_{l_e} \mathbf{B}_w^T \mathbf{a}_w^T \mathbf{K}_m \mathbf{a}_w \mathbf{B}_w dx \end{aligned} \quad (19)$$

\mathbf{P}_e being the internal element force vector:

$$\mathbf{P}_e = \begin{bmatrix} \int_{l_e} \mathbf{B}_p^T \mathbf{a}_s^T \hat{\sigma}(\epsilon^P, \epsilon^w) dx \\ \int_{l_e} \mathbf{B}_w^T \mathbf{a}_w^T \hat{\sigma}(\epsilon^P, \epsilon^w) dx \end{bmatrix} \quad (20)$$

Considering \mathbf{K}_m as the stiffness tangent operator, the linearized form of the stress vector $\hat{\sigma}$ is defined as:

$$\hat{\sigma}(x, y) = \mathbf{K}_m \epsilon = \mathbf{K}_m (\epsilon^P + \epsilon^w) \quad (21)$$

On the other hand, each cross section is discretized into n_s 6 nodes triangular elements. Therefore the section stiffness matrix and the sectional force vector are expressed as follows:

$$\mathbf{P}_s = \sum_{S^e=1}^{n_s} \begin{bmatrix} \int_{S^e} \mathbf{a}_s^T \hat{\boldsymbol{\sigma}}(\epsilon^P, \epsilon^w) dS^e \\ \int_{S^e} \mathbf{a}_w^T \hat{\boldsymbol{\sigma}}(\epsilon^P, \epsilon^w) dS^e \end{bmatrix} = \begin{bmatrix} \mathbf{P}_{sp,c} \\ \mathbf{P}_{sw,c} \end{bmatrix} \quad (22)$$

$$\mathbf{K}_s = \sum_{S^e=1}^{n_s} \begin{bmatrix} \mathbf{K}_{spp} & \mathbf{K}_{spw} \\ \mathbf{K}_{swp} & \mathbf{K}_{sww} \end{bmatrix} = \begin{bmatrix} \mathbf{K}_{spp,c} & \mathbf{K}_{spw,c} \\ \mathbf{K}_{swp,c} & \mathbf{K}_{sww,c} \end{bmatrix} \quad (23)$$

Where:

$$\begin{aligned} \mathbf{K}_{spp} &= \int_{S^e} \mathbf{a}_s^T \mathbf{K}_m \mathbf{a}_s dS^e \\ \mathbf{K}_{spw} &= \int_{S^e} \mathbf{a}_s^T \mathbf{K}_m \mathbf{a}_w dS^e \\ \mathbf{K}_{swp} &= \int_{S^e} \mathbf{a}_w^T \mathbf{K}_m \mathbf{a}_s dS^e \\ \mathbf{K}_{sww} &= \int_{S^e} \mathbf{a}_w^T \mathbf{K}_m \mathbf{a}_w dS^e \end{aligned} \quad (24)$$

For all the integral calculations, the Gaussian quadrature is applied.

4 IMPLEMENTATION OF LONGITUDINAL AND TRANSVERSAL REBARS

In the case of reinforced concrete elements, the contribution of the longitudinal rebars must be added to that of the concrete fibers. The total section will thus be represented by the sum of the concrete area and the section of the longitudinal reinforcement. The latter one is modelled as point elements intersecting the concrete cross-section. The shape and dimensions of the bar are considered as negligible. Consequently, the warping and distortion of this point element are not taken into account. It follows that the deformations of these elements are composed only by the terms of the plane strain field ϵ^P defined by Timoshenko's theory.

Regarding the implementation of stirrups, they are modelled as bar elements with linear elastic constitutive law. Each leg of the transversal rebars is discretized into n_{st} sub-elements of length l_{st} , presenting two nodes where the transversal distortional displacements components u_y^w and u_z^w are computed as presented by Figure 4.

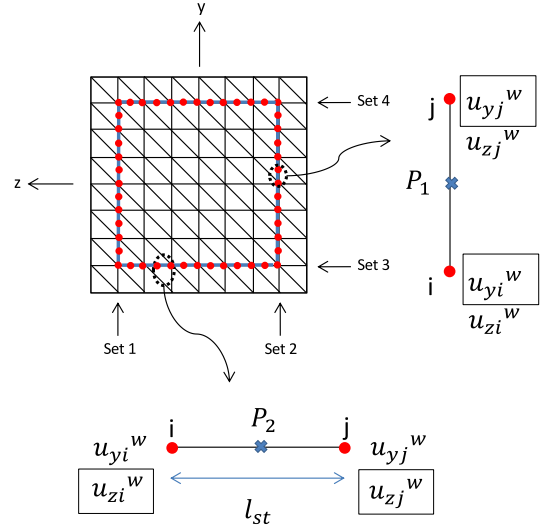


Figure 4: Cross-section discretization: concrete and transversal steel reinforcement mesh

Linear Lagrange polynomials N_1 and N_2 are used to interpolate distortion between these two nodes at a single integration Gauss point P. All transversal sub-element rebars colinear to y-direction belong to (Set 1) or (Set 2), whereas those towards z-direction are attributed to (Set 3) and (Set 4) as seen in Figure 4.

If a Gauss point P_1 belongs to (Set 1) or (Set 2), its total displacement $u_{st}^w(P_1)$ has only one distortional component in y-direction interpolated as follows:

$$u_{y,st}^w(P_1) = N_1 u_{y,i}^w + N_2 u_{y,j}^w \quad (25)$$

As for (Set 3) and (Set 4), a single transversal component along z-axis is assigned to the displacement field $u_{st}^w(P_2)$ such as:

$$u_{z,st}^w(P_2) = N_1 u_{z,i}^w + N_2 u_{z,j}^w \quad (26)$$

Having the expression of the displacement at points P_1 and P_2 , the enhanced transversal strain can be deduced.

On the other hand, the contribution of the transversal rebars can be seen at the sectional level, with extra terms added to \mathbf{P}_s and \mathbf{K}_s such that:

$$\mathbf{P}_s = \begin{bmatrix} \mathbf{P}_{sp,c} \\ \mathbf{P}_{sw,c} + \mathbf{P}_{sw,st} \end{bmatrix} \quad (27)$$

$$\mathbf{K}_s = \begin{bmatrix} \mathbf{K}_{spp,c} & \mathbf{K}_{spw,c} \\ \mathbf{K}_{swp,c} & \mathbf{K}_{sww,c} + \mathbf{K}_{sww,st} \end{bmatrix} \quad (28)$$

All the components of the sectional force vector \mathbf{P}_s and stiffness matrix \mathbf{K}_s with indices c related to concrete fibers are expressed by equations ((22),(23) and

(24)). On the other hand, $\mathbf{P}_{sw,st}$ and $\mathbf{K}_{sww,st}$ referring to transversal steel reinforcements are defined as follows:

$$\begin{aligned}\mathbf{P}_{sw,st} &= \sum_{e=1}^{N_{st}} \int_{\Omega^e} A_{st} \times \mathbf{a}_{w,st}^T \times \boldsymbol{\sigma}_{st} d\Omega^e \\ \mathbf{K}_{sww,st} &= \sum_{e=1}^{N_{st}} \int_{\Omega^e} A_{st} \times \mathbf{a}_{w,st}^T \times \mathbf{E}_s \times \mathbf{a}_{w,st} d\Omega^e\end{aligned}\quad (29)$$

A_{st} , N_{st} and E_s being respectively the area of transversal rebars, the total number of transversal steel sub-elements and the steel tangent stiffness.

Also, in order to attribute a realistic value for the transversal reinforcement area A_{st} , an analogy is done between the enhanced numerical model and a realistic representation of a reinforced concrete beam confined with stirrups equally distributed with a spacing denoted s . Figure 5 presents the analogy made between the numerical beam element and a realistic reinforced concrete beam. Therefore, the adequate nu-

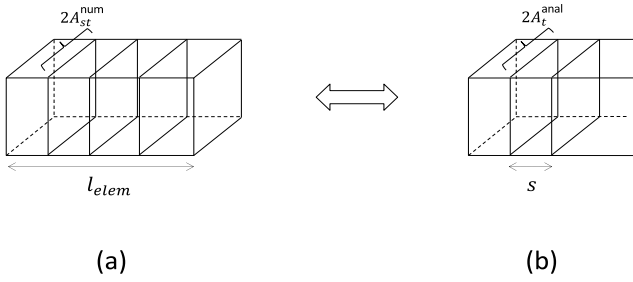


Figure 5: Analogy between a multifiber element presenting 3 sections (a) with a realistic representation of a reinforced concrete beam confined with stirrups (b)

merical rate of stirrups per meter can be obtained by applying the following analogy:

numerical model	analytical representation
$\frac{A_{steel}^{num}}{l_e} = \frac{2 \times A_{st}^{num} \times n_{section}}{l_e}$	$\frac{A_{steel}^{anal}}{s} = \frac{2 \times A_t^{anal}}{s} = \frac{2 \times \pi d^2}{s \times 4}$
$\Leftrightarrow \frac{2 \times A_{st}^{num} \times n_{section}}{l_e} = \frac{2 \times A_t^{anal}}{s}$ (30)	

Hence, the section of transversal steel, A_{st}^{num} , that should be implemented in the numerical model is obtained:

$$A_{st} = A_{st}^{num} = \frac{A_t \times l_e}{n_{section} \times s} \quad (31)$$

$n_{section}$ being the notation used to refer to the number of sections per element of length l_e in the discretized multifiber beam.

5 VALIDATION PROCESS: NUMERICAL CASE STUDIES

5.1 Linear elastic cantilever beam without stirrups

The enhanced multifiber beam element is validated by performing tension and flexure tests on a plain concrete cantilever beam in the linear elastic range. It's a beam of length $L = 1$ m, modelled using 11 Timoshenko multifiber elements, each having 3 Gauss points. The dimensions of the selected cross-section which is meshed using TRI6 triangular elements are represented in Figure 6. Concrete is modelled using a

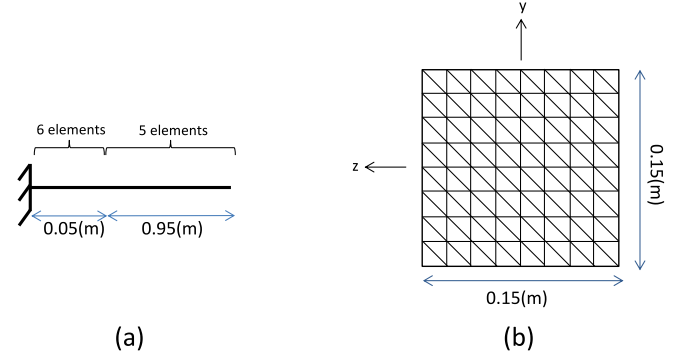


Figure 6: Longitudinal beam element discretization (a). Cross-section description (b).

3D linear elastic constitutive law and the stress-strain relations are defined as follows :

$$\boldsymbol{\sigma} = \frac{E}{1 + \nu} \left[\boldsymbol{\epsilon} + \frac{\nu}{1 - 2\nu} Tr(\boldsymbol{\epsilon}) \mathbf{I} \right] \quad (32)$$

The efficiency of the proposed modelling strategies is tested by confronting the numerically obtained results with those of a standard 3D finite element model. To this end, a 3D cantilever beam was meshed with tetrahedral elements. All the computational analysis for both types of models was performed using the library ATLAS (A Tool and Language for Simplified Structural Solution Strategy) developed on the Matlab platform at INSA-Lyon by Prof. S. Grange.

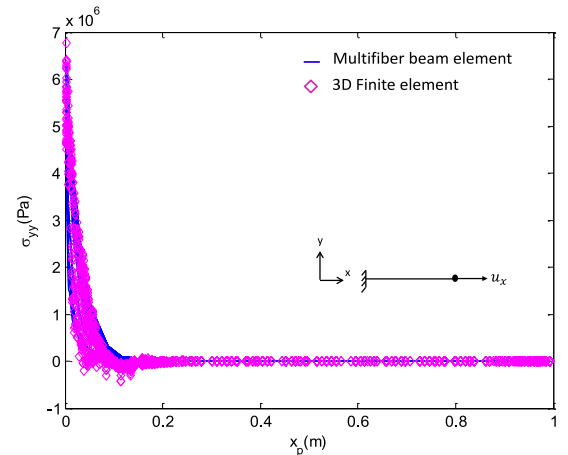


Figure 7: Tension test: Variation of transversal stresses σ_{yy} with respect to the length of the beam

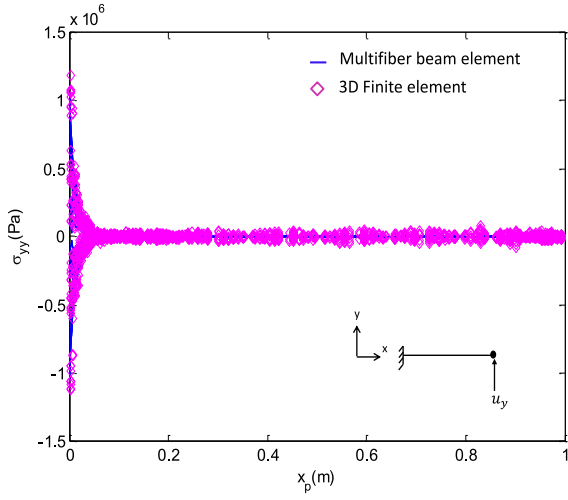


Figure 8: Flexion test: Variation of transversal stresses σ_{yy} with respect to the length of the beam

The first aim of the verification process is achieved by plotting the variation of normal transversal stresses σ_{yy} computed at each Gauss point of the cross-section with respect to the beam length as seen in Figure 7 where a tension test is simulated and Figure 8 which displays the outcomes of a simple flexure test. In both cases, all the enhanced degrees of freedom are restrained at the fixed end, the reason why high gradients of σ_{yy} are observed at this location of the beam. As for the free end, $u_x = 1\text{mm}$ and $u_y = 1\text{mm}$ are applied in order to perform respectively the tension (Figure 7) and bending (Figure 8) tests. The beam is free to distort at the free end, hence, the value of σ_{yy} tends to zero. The numerically obtained outcomes prove that the equilibrium state is reached, and a good matching between the results obtained with the 3D enhanced multifiber model and the 3D finite element solution.

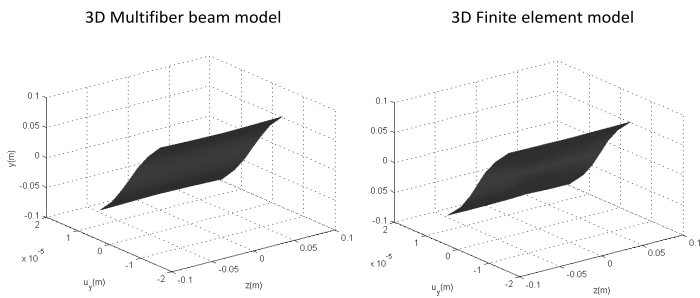


Figure 9: Tension test: Transverse displacement maps obtained with the 3D enhanced multifiber model and the standard 3D FE model

Moreover, transversal displacement u_y maps are displayed in Figures 9 and 10. By confronting the results provided by the proposed model with those coming from a standard 3D finite element formulation, good agreement can be observed showing the efficiency of the proposed model in reproducing displacements, strains and stresses in the linear elastic framework.

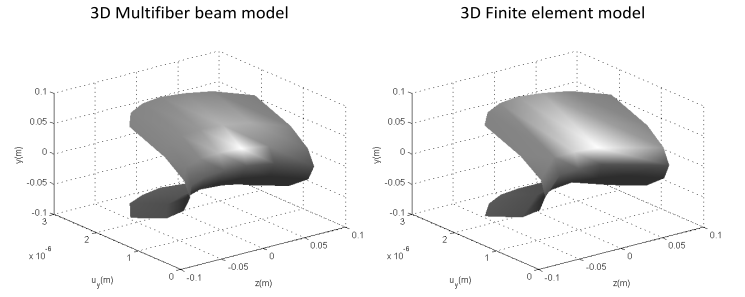


Figure 10: Flexion test: Transverse displacement maps obtained with the 3D enhanced multifiber model and the standard 3D FE model

5.2 Concrete beam element confined with stirrups

This section highlights the role of stirrups on confining concrete fibers. To this end, dilation effect is simulated by imposing a thermal dilation effect to the concrete fibers in the linear elastic phase. By applying this method and with a large section of stirrups confining the concrete fibers, the initial and deformed shapes of the cross-section are presented in Figure 11. Also, it can be seen in Figure 12 that the comparison between the proposed multifiber model and the 3D FE model presents a reasonable agreement in terms of transversal displacement maps.

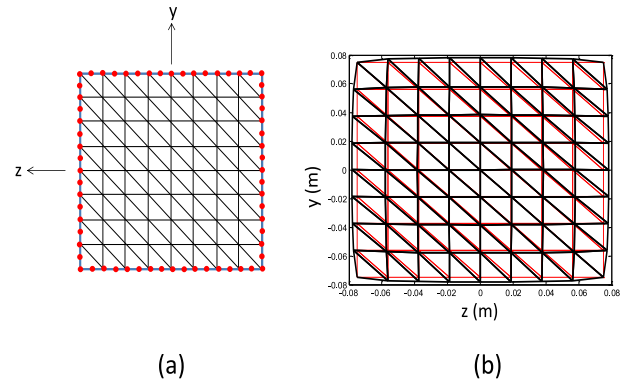


Figure 11: Concrete section confined with stirrups (a). Initial (red) and deformed (black) shape of the cross-section (b).

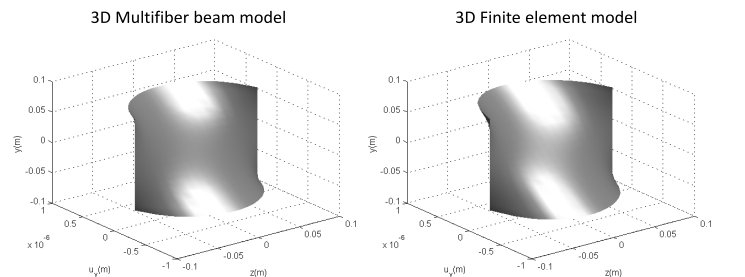


Figure 12: Transverse displacement maps for concrete fibers confined by large section of stirrups

6 CONCLUSION

An efficient 3D multifiber beam model was presented aiming at reproducing the vertical stretching of the concrete cross-section confined by stirrups. This distortional effect is taken into account by adding new degrees of freedom to the global level. A novel Timoshenko beam element recently developed by Caillerie et al. (2015) for 2D applications, has been chosen and extended in our model to the 3D formulation in order to avoid shear locking problems. Also, it should be mentioned that the present formulation of the section equilibrium is derived from the one presented by Capdevielle et al. (2016) which takes into account the warping of the cross-section.

The presented model is suitable for an arbitrary cross-section and material. Its efficiency is highlighted by comparing the numerically obtained results in terms of stresses and displacement with those coming from 3D finite element modelling. Good matching was observed showing the robustness of the enhanced model and validating its performance in the linear elastic phase.

Furthermore, longitudinal and transversal rebars are modelled. Their implementation was validated by introducing a dilatancy effect to the concrete fibers and confronting the obtained outcomes with those coming from a 3D FE model.

The case studies investigated herein are related to static loadings, although cyclic loadings can take place. A nonlinear dilatant constitutive law is to be implemented and tested on reinforced concrete elements under monotonic and cyclic loadings and hence study the nonlinear response of structural concrete elements subjected to transverse shear. Also, the mass matrix can be implemented in order to conduct dynamic simulation studies, and the warping effect, taken into account by Capdevielle et al. (2016), can be coupled with the distortion of the section in order to obtain a complete 3D enhanced multifiber beam model.

REFERENCES

- Caillerie, D., P. Kotronis, & R. Cybulski (2015). A timoshenko finite element straight beam with internal degrees of freedom. *International Journal For Numerical And Analytical Methods In Geomechanics* 39, 1753–1773.
- Capdevielle, S., S. Grange, F. Dufour, & C. Desprez (2016). A multifiber beam model coupling torsional warping and damage for reinforced concrete structures. *European Journal of Environmental and Civil Engineering* 20, 914–935.
- Cusson, D. & P. Paultre (1995). Stress-Strain model for confined high-strength concrete. *Journal of Structural Engineering* 121, 468–477.
- Guedes, J., P. Pegon, & A. Pinto (1994). A fibre/timoshenko beam element in castem 2000. *Applied Mechanics Unit, Safety Technology Institute, Joint Research Center, European Commission, I-21020 Ispra(VA) Italy, Special Publication Nr. I.94.31*.
- Ibrahimbergović, A. & F. Frey (1993). Finite element analysis of linear and non-linear planar deformations of elastic initially

curved beams. *International Journal for Numerical Methods in Engineering* 36, 3239–3258.

Le Corvec, V. (2012). *Nonlinear 3d frame element with multi-axial coupling under consideration of local effects*. Ph. D. thesis, University of California, Berkeley.

Mohr, S., J. Bairàn, & A. Mar (2010). A frame element model for the analysis of reinforced concrete structures under shear and bending. *Engineering structures* 32, 3936–3954.

Stolarski, H. & T. Belytschko (1982). Membrane locking and reduced integration for curved elements. *Journal of Applied Mechanics* 49, 172–176.